Microdroplet-Based Organic Vapour Sensor on a Disposable GO-Chitosan Flexible Substrate

Mitradip Bhattacharjee, *Member, IEEE*, Anastasios Vilouras, *Student Member, IEEE*, and Ravinder Dahiya, *Fellow, IEEE*

***Abstract*—With rising hazardous organic vapours in the environment, the detection of volatile organic vapour compounds (VOCs) is becoming important. To this end, this paper presents a conductive droplet-based disposable sensor. Unlike conventional sensors, the droplet system is easily replaceable and is capable of detecting multiple vapours based on surface tension gradient. The chemiresistive sensor presented here is fabricated on 2.5 μm thick ultra-flexible graphene oxide-chitosan (GOC) with Pt electrodes having 60 μm gap. The electrostatic interaction and strong hydrogen bonds between GO and polysaccharide groups in chitosan provide tunable hydrophobicity and stability to the droplet. With a conductive droplet of ~10 μL of aq. NaCl as an active sensing material dispensed between the Pt electrodes, it was observed that the droplet showed 14-21% change in resistance in the presence of VOCs. A read-out circuit was also designed to get the data from the droplet sensor. The response time for the presented sensor (3-4 seconds) is significantly better than its solid-state sensor counterparts. With attractive features such as disposability, affordability and fast response the presented sensor will find applications in industrial environments, laboratories, health centres, and biomedical devices.**

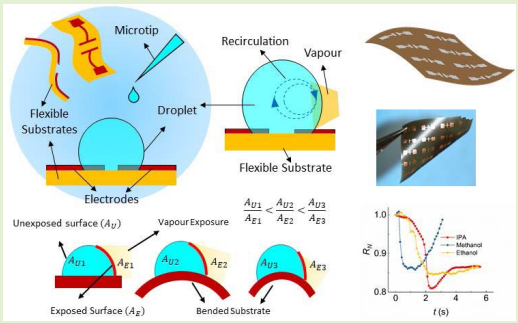

***Index Terms*— Disposable sensors, printed electronics, microfluidics, VOC.**

I. Introduction

MICROFLUIDIC sensing systems are employed extensively in various sensing applications due to the ease of fabrication, and control of fluid [1], [2]. As a result, these systems have gained popularity in applications based on microelectronics [3], [4], biosensing [5], stretchable electronics [6], and microelectromechanical systems [7]. With electronic [8], optical [9] and mechanical systems [10], the microfabricated channels and pumps have been employed to obtain highly sensitive devices and sensors. Paper based microfluidic sensors, with possibility of easy disposal have also been reported in the literature [11], [12]. Although these systems offer features such as low-sample requirement, higher sensitivity, and precise control of flow and heat, they suffer from the inability to create patterned motions inside the system. Several methods have been utilized to overcome the problem such using high electric fields and an alternative approach of using droplet-based microfluidics [13]. But, most of them require high electric field or substantial external influence. In this regard, the droplet-microfluidics has gained interest as it is relatively simple and does not require a fluid-flow arrangement.

Droplet-microfluidics are mostly based on a microdroplet rather than a flowing system [14]. The volume of the droplets can be tuned from microliter to femtoliter based on the requirement and hence the requirement of sample is also very low. The small droplets can be controlled by microstructures with relatively fewer requirements of external energy and lead to highly sensitive sensors. Further, this approach provides an opportunity to encapsulate a large number of target molecules in a single droplet system and hence to analyse the large data by splitting, merging, and sorting of the droplets through the application of external stimulations. Exploiting these advantages, here we present a conductive droplet-based disposable sensor for detection of volatile organic vapour compounds (VOCs). With rising hazardous organic vapours in the environment, the detection of VOCs is important for human safety.

The conductive droplet-based disposable VOC sensor presented here shows the response time of 3-4 seconds, which is significantly better than the widely used solid-state sensors, as explained later. The chemiresistive sensor used in this work

Manuscript received March 31, 2020; revised April 24, 2020; accepted April 30, 2020. Date of publication May 4, 2020; date of current version June 18, 2020. This work was supported in part by the EPSRC Engineering Fellowship for Growth under Grant EP/R029644/1 and Grant EP/M002527/1, and in part by the North West Centre for Advanced Manufacturing (NW CAM) project supported by the European Union's INTERREG VA Programme, managed by the Special EU Programmes Body (SEUPB) under Grant H2020-Intereg-IVA5055. The associate editor coordinating the review of this article and approving it for publication was Prof. Sang-Seok Lee. *(Corresponding author: Ravinder Dahiya.)*

The authors are with the Bendable Electronics and Sensing Technologies (BEST), University of Glasgow, Glasgow G12 8QQ, U.K. (e-mail: ravinder.dahiya@glasgow.ac.uk).

Digital Object Identifier 10.1109/JSEN.2020.2992087

is fabricated on 2.5 μm thick ultra-flexible graphene oxide-chitosan (GOC) with Pt electrodes which are 60 μm apart. The presence of GO in the GOC substrate provides the optimum hydrophobicity to the droplet for efficient operation. The electrostatic interaction and strong hydrogen bonds between GO and polysaccharide groups in chitosan provide tunable hydrophobicity and stability to the droplet. Moreover, the biocompatibility and bioresorbability of GOC substrate are highly desirable features in the disposable sensing applications. With a conductive droplet ($\sim$10 μL of aq. NaCl as an active sensing material) dispensed between the Pt electrodes, the resistance of droplet shows 14-21% change in the presence of VOCs. Unlike conventional sensors, the droplet system is easily replaceable and is capable of detecting multiple vapours based on surface tension gradient. Droplet-based sensors [14], [15] also provides the additional advantage of being reused with minimum physical interventions. The work presented in this paper extends our previous work presented at IEEE FLEPS 2019 conference [16]. With respect to the preliminary work presented in the conference, herein we have further analysed the sensors for stability and for the effect of bending. Further, the circuit implementation is presented for the VOC sensor.

This paper is organised as follows: Section II briefly presents the state of the art related to VOC sensors. The materials and methods related to the presented droplet-based VOC sensor are described in Section III. This is followed by the analysis of results in Section IV and circuit details in Section V. Finally, the key outcomes are summarised in Section VI.

II. State of the Art

Over the past few decades, a number of organic vapour sensors have been developed utilizing various materials such as metal-oxide, carbon materials, and polymer composites, etc. [17], [18]. Many of these sensors require high operating temperature and are unsuitable for multiple vapour detection. The deteriorated performance of many of the existing sensors during prolonged exposure of vapour is another issue which renders them useless after some time. A replaceable and disposable sensor can provide the solution in such a scenario. Recently, solid-state metal-oxide sensors have been explored to overcome such issues, but currently, they are not economic [19]–[25] and hence not attractive for disposable applications. Moreover, multiple uses of a sensor for different users create the concern of hygiene. These challenges are driving the research towards the development of affordable, flexible, and disposable sensors [26], [27]. As a result, sensors on flexible substrates are being explored for detection of pH [28], [29], temperature [30], and body-fluid [28] etc. Other examples include, VOC sensors based on self-assembled nanoparticles produced by a droplet of colloid [31]. Many of these sensors perform better when compared to their conventional solid-state counterparts. A performance comparison is shown in Table I. Further, being flexible, these sensors can conform to curvy surfaces and have the advantage of being suitable for wearable applications. However, disposability of these sensors has not attracted much attention. In this regard, our recent works on sensors are relevant as we demonstrate the biodegradibility and hence suitability of GOC based sensors for the disposable application [32], [33]. With the droplet sensing mechanism, if needed, it is possible to reuse the sensors on GOC substrates for a few tests. Droplet being the active material, the sensor can be used a few times just by replacing the previous droplet with a new one. The droplet system also shows better response time, as discussed in the following sections. Microfluidics based sensors are gaining attention for their ease of implementation. In this line, many droplet-based sensors [15], [34], [35] have been reported for a variety of applications but these are not compatible with wearable systems. Hence, droplet sensors on a flexible substrate could open new avenues in bendable electronics.

TABLE I
PROPERTIES OF THE VOCS UNDER CONSIDERATION

VOC	Surface Tension, γ (mN/m)	Surface Tension Gradient*, $\Delta\gamma$ (mN/m)	Diffusivity in water (cm^2/s)	Diffusivity in air (cm^2/s)
IPA	20.7	51.3	1.03×10^{-5}	0.0959
Ethanol	21.66	50.34	1.15×10^{-5}	0.115
Methanol	21.79	50.21	2.63×10^{-5}	0.15

*The gradient was measured w.r.t. water (72 mN/m)

III. Materials and Methods

A. Materials

Graphene oxide (GO) (ultra-high concentrated single-layer graphene oxide solution, 6.2 g/l) procured from Graphene Supermarket, US. Cellulose acetate butyrate (CAB), chitosan, ethyl-L-lactate, acetic acid, iso-propyl alcohol (IPA), methanol, ethanol has been procured from Sigma Aldrich, UK. All chemicals were used as procured.

B. Fabrication Process

The fabrication process of the flexible chemiresistive sensor is similar to the one reported previously [32], [36], [37]. The GOC composite was synthesized by dissolving 2mL of GO solution, 0.5 g of Chitosan, and 4.5mL of 2% acetic acid in 50 mL of DI water. The solution was stirred vigorously at 40° C using magnetic stirrer at 1300 rpm for 12 hrs to disperse GO and completely dissolve chitosan. Subsequently, 5% (wt. %) cellulose acetate butyrate (CAB) was dissolved in ethyl-L-lactate and spun on a silicon substrate at 1000 rpm for 30 seconds. Then the synthesized GOC composite was drop-casted on silicon substrate pre-coated with CAB. Here the CAB acts as a sacrificial layer and prevents any fabrication induced damage of the GOC film. The major fabrication steps are shown in Fig. 1(a). The Pt electrodes (separation gap - 60μm) were then deposited on the GOC flexible film using a hard-mask. The fabricated flexible substrate and the microscopic image of the electrodes are shown in Fig. 1(b) and 1(c) respectively. The electrostatic interaction and strong hydrogen bonds between GO and polysaccharide groups in chitosan provide tunable hydrophobicity and stability to the droplet. Moreover, GOC has attractive features such as

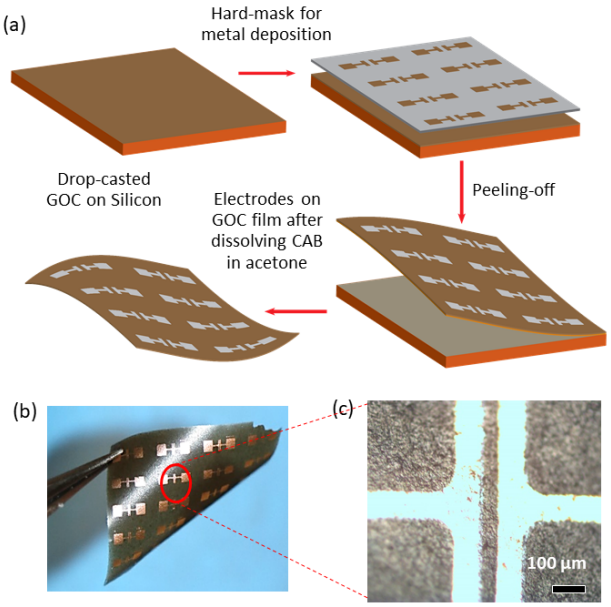

Fig. 1. (a) Fabrication steps; (b) optical images the fabricated electrodes on flexible substrate; and the (c) optical microscopic image of the fabricated electrode.

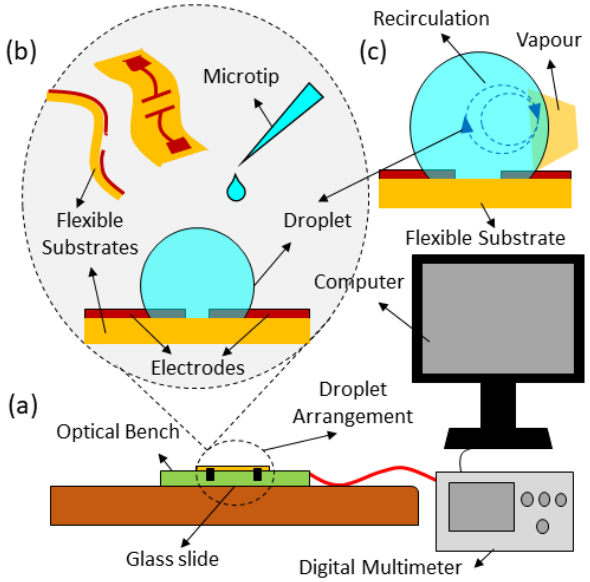

Fig. 2. (a) The scheme of the experimental set-up; (b) the schematic illustration of droplet set-up on flexible substrate; (c) the scheme of Marangoni circulation due to exposure of vapour near the droplet surface.

disposability, affordability, biocompatibility and bioresorbability which makes it suitable for this application.

C. Characterisation

The experiment was carried out with a sessile conductive droplet of 1.7M aq. NaCl salt solution after optimising the concentration of NaCl. The salt solution of different concentration was prepared at room temperature. Initially, a droplet of ~10 μl was dispensed in between a pair of Pt electrodes deposited on the GOC substrate. Fig. 2(a) and 2(b) describe the set-up employed for the experiments. The electrodes were connected

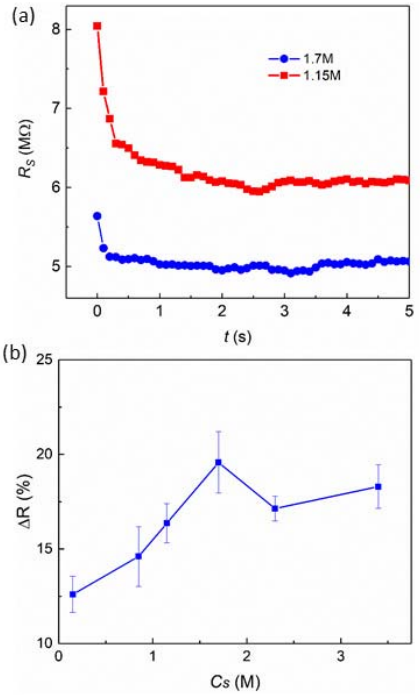

Fig. 3. (a) The electrical stability response (R_S) of the aq. NaCl (conc. 1.7M and 1.15M) droplet in an ambient condition, (b) the response of the sensor for different salt concentration (C_S) of NaCl.

to the digital multimeter (Agilent 34461A) to record the electrical resistance across the droplet as shown in Fig. 2(a). In order to characterize the effect of VOCs, another droplet of an organic vapour was kept at a distance of ~1 cm and the electrical response was recorded. In another approach, the vapour source was introduced using micropipette. Fig. 2(c) shows the schematic of induced Marangoni motion inside the droplet due to the introduction of vapour which creates a surface tension gradient on the droplet surface. The material characterisation of the substrate has been performed and reported in our previous work [33].

IV. Results and Discussions

The droplet on the flexible substrate was electrically characterized in ambient condition inside the laboratory in a calm environment. It was observed that after dispensing the droplet, it took 1-2 seconds for the droplet to stabilize electrically, as can be noted from Fig. 3(a). This is because it takes some time for mechanical stability. An experiment was performed with IPA as vapour source at different concentration of NaCl and the maximum response was observed at 1.7M of NaCl as illustrated in Fig. 3(b) and thus further experiments were performed with 1.7 M of NaCl solution. The decrease in the response at lower and higher concentration can be attributed to the low conductance of the solution and increase in the density and viscosity that restricts the Marangoni rotation inside the fluid, [14] respectively. Further, the normalized resistance, $R_N (= R/R_0$, where R_0 is the base resistance of the droplet) across the droplet decreased by 14-21%, (Fig. 4(a)) due to the presence of different organic vapours (i.e. isopropyl alcohol (IPA), methanol, and ethanol). Fig. 4(a) shows the

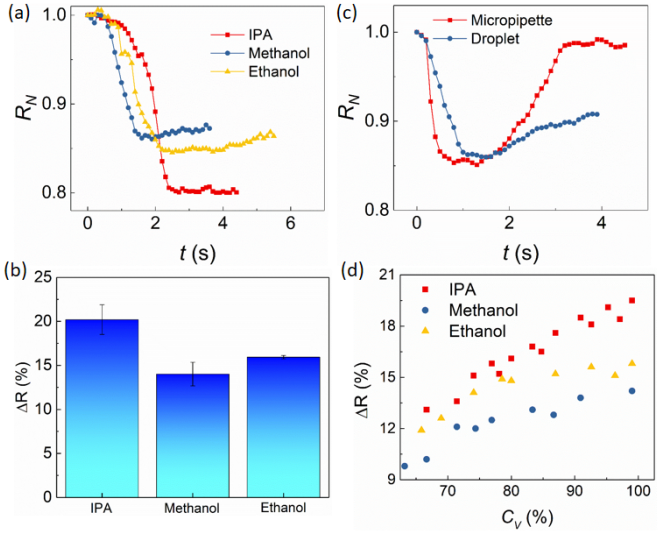

Fig. 4. (a) Temporal sensor response in presence of IPA, methanol, and ethanol, (b) the percentage change in resistance for IPA, methanol, and ethanol, (c) temporal response of the sensor for methanol exposure in two experimental conditions, (i) placing a drop of methanol near the sensor (droplet), (ii) introducing methanol using micropipette (micropipette), (d) the response of the sensor for different concentration of vapours.

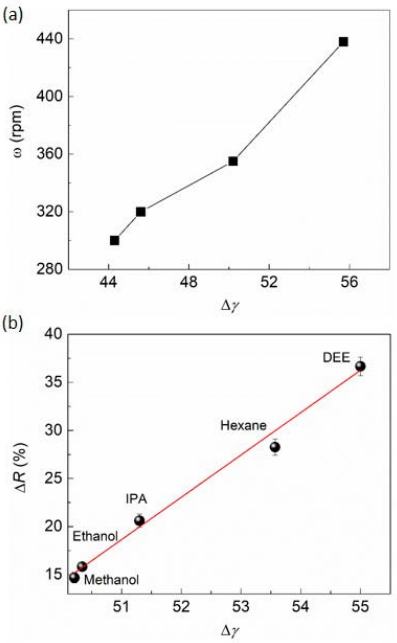

Fig. 5. (a) Change in the rotational motion (ω) with the surface tension gradient ($\Delta\gamma$), (b) response with the gradient of interfacial tension between the air-water and vapour-water interfaces. The error bars are the standard deviation of at least 3 repeated measurements.

stabilised signal from the sensor for the mentioned three vapours. The percentage change in resistance (ΔR) for each vapour is shown in Fig. 4(b). The signal of the sensor for two different experimental conditions, (i) placing a drop of methanol near the sensor (indicated as "droplet" in Fig. 4(c)), (ii) introducing methanol using micropipette (indicated as "Micropipette" in Fig. 4(c)), was recorded as illustrated in Fig. 4(c). In case of droplet of VOC, the sensor signal was not recovered to its initial value since the VOC drop takes time to evaporate completely, whereas, pulsed introduction of vapour using micropipette for a few seconds (1-2 s) demonstrated almost a complete recovery. Further, the experiment performed for Fig. 4(c) also showed that the recovery of the sensor was good and further the response of the sensor is not influenced by the droplet of vapour as it also illustrated similar response for vapour in micropipette. Fig. 4(d) shows the response of the sensor for different concentration (60 – 100%) of vapours. As the targeted application of the sensor is the detection of alcohol intoxication from breath analysis or leakage at industrial areas or laboratories, the concentration under consideration is apt for the same. The response of the sensor was found to be higher for higher surface tension gradient between the vapour-water and air-water interface. Each VOC has their specific surface tension as listed in Table I and hence will produce a specific response based on the surface tension gradient upon exposure. The surface tension gradient creates the recirculation inside the droplet due to the Marangoni effect which in turn increases the conductance across the droplet. A two-dimensional computational fluid dynamic simulation was performed in COMOSOL Multiphysics in order to study the rotational strength (ω) inside the fluid due to surface tension gradient by solving Navier–Stokes equations for a two-phase system with suitable boundary conditions as reported in our previous work [14] The simulation result shows that the rotational motion in the droplet increases with the surface tension gradient ($\Delta\gamma$) as illustrated in Fig. 5(a). Thus, the change in the sensor response (ΔR) is higher for higher surface tension gradients. Similar response was also reflected in the experimental results and the ΔR is correlated with the surface tension gradient ($\Delta\gamma$) between the water-air and water-organic vapour interface as shown in Fig. 5(b) for five VOCs (ethanol, methanol, iso-propyl alcohol (IPA), hexane, and diethylether (DEE)). The surface tension gradient can also be correlated with vapour pressure however the two are related to each other [38], [39] The response of the sensor for three different vapours shows different rates of change which is due to diffusivity of three vapours in air and water. The diffusivity of IPA is lowest compared to ethanol, and methanol as illustrated in Table I. Hence, it takes long time for IPA to reach the sensing surface and diffuse into the droplet. This reflected by IPA's lowest rate of change or highest response time (~2.4 s) among these three mentioned vapours as shown in Fig. 4(a). Similarly, methanol showed the fastest response (~1.4 s) than IPA and ethanol (~2.1 s). The sensor, in this case, is disposable and it was chemically stable on the GOC substrate up to 2-3 times of use as discussed later.

The experiments were also performed to understand the stability of the sensors for different cycles of experiments as shown in Fig. 6(a). These experiments were performed by repeating the measurements on a single substrate. The droplet was removed from the substrate after each measurement using a water absorbent paper and a new droplet was introduced for the measurement. It was observed that the sensor is usable for 3 consecutive times. Thereafter, in most of the cases,

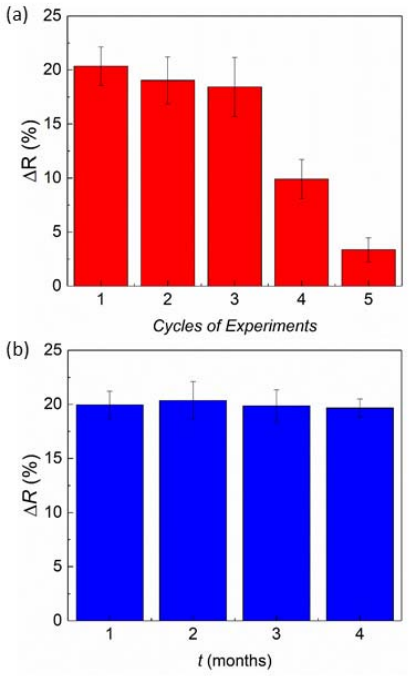

Fig. 6. Response of same sensor patch with (a) repeated cycle of experiments and (b) repeated tests at different time with same batch of sensor patch to check the stability of the sensor patch.

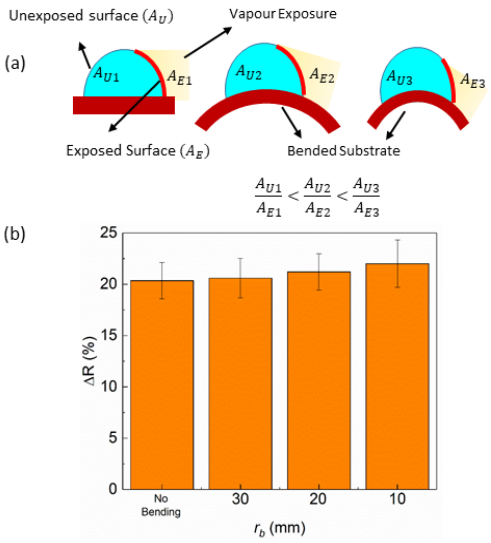

Fig. 7. Response of same sensor under bending conditions. (a) schematic illustration in static bending condition, (b) response of the sensor for different bending radius.

the substrate got degraded, and the electrodes got damaged. However, the fabricated sensor patches are quite stable in terms of storage. As an example, a single batch of sensor was stored for more than four months and it was found that the sensors showed stable response, as shown in Fig. 6(b). In this case, a sensor was used from a batch for one measurement and then discarded. Thereafter, a sensor fabricated in the same batch was employed for the experiments at regular time interval.

Further experiments are carried out to evaluate the effect of static bending during usage. The motion inside the droplet depends on the exposure of VOC on the surface of the droplet. During bending the effective ratio between unexposed (A_U) to exposed (A_E) surface area increases that forms localised surface tension gradient and hence the influence of vapour is more prominent. The unexposed surface area increases with the higher bending and thus the ratio (A_U/A_E) increases as illustrated schematically in Fig. 7(a). The sensor, in this case, was tested for 30-10 mm bending radii. The sensor was mounted on three different 3D printed bending set-up having 10, 20, and 30 mm bending radii. Thereafter the IPA vapour was introduced and the electrical response was recorded using a digital multimeter as explained previously. Fig. 7(b) shows the effect of bending on the sensor response. As described, the higher bending (low bending radius) resulted in a higher response of the sensor. This means the response could be modulated by bending the substrate.

V. Circuit Details

Chemi-resistive method of detection is widely used in a variety of application including medical and industrial electronics. In general, the resistance of gas (e.g. hydrocarbons, propane, methane) and VOC (e.g. alcohols) sensors vary from several Ohms to several Mega-Ohms depending on the sensing material and the biasing conditions. Normally an analogue front-end followed by an analogue-to-digital converter (ADC) is interfaced with the sensor in order to digitize the change in resistance. A simple way to convert the change in the resistance to voltage and then to digitize is to use a voltage divider or a Wheatstone bridge configuration followed by an operational amplifier to step-up the analogue sensor signal and reduce the offset voltage before sending it to an ADC to digitize the same. However, depending on the application requirements, these implementations have inherent measurement limitations, which can be device or sensor specific. The main reason is that the response of chemi-resistors exhibits a logarithmic relationship between the sensor's resistivity and gas or vapour concentration. This relationship is an expression as: $R_{sens} = A \cdot C^{-a}$, where R_{sens} is the resistance of the sensor, C is the gas concentration, and A and a are two constant factors. Therefore, in a voltage divider configuration, the output voltage will not be linear, and it will follow the Eq. (1) below:

$$log\left(V_{out}/V_{in}\right) = log\left(\frac{R_{Fixed}}{R_{Fixed} + A \cdot C^{-a}}\right) = log\left(R_{Fixed}\right) - log\left(R_{Fixed} + A \cdot C^{-a}\right) \quad (1)$$

where, R_{Fixed} is the fixed resistance of the voltage divider. Therefore, this approach can be used for applications that require gas detection rather than a precise quantitative measurement of the concentration.

For applications requiring precise measurement, the circuit highlighted with a dashed blue line in Fig. 8(a) can be used by applying a constant input voltage (V_{in}). This circuit can be used in other chemiresistive applications; however, it is designed specifically for the proposed sensor for VOCs detection. The post-layout simulation was performed for the said

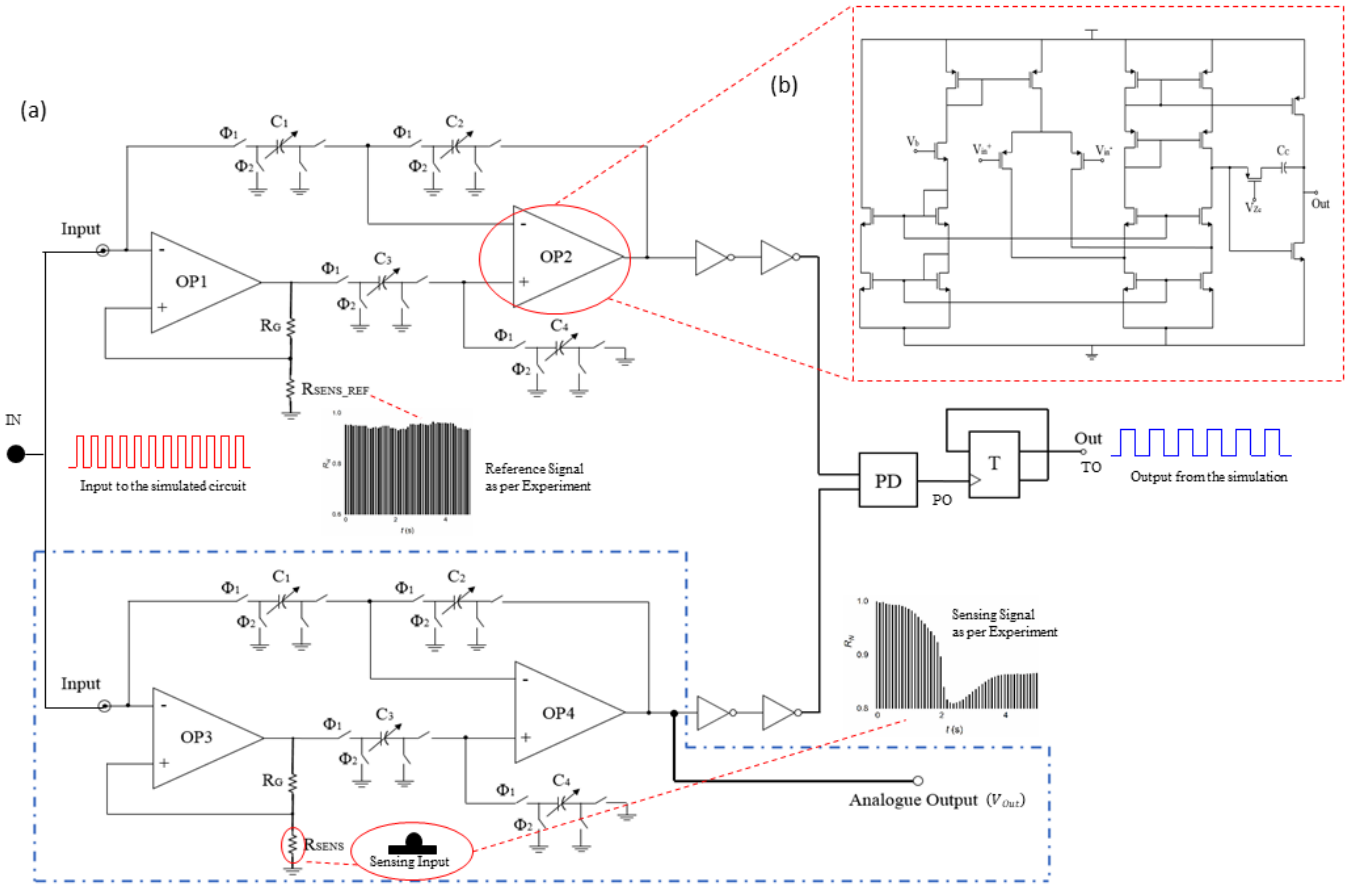

Fig. 8. (a) Block diagram of the proposed chemiresistance-to-frequency converter. The blue dashed line highlights the analogue front-end that can be used by applying a constant input voltage (V_{in}). (b) The schematic of the two-stage folded cascade amplifier used in OP 1 - 4.

circuit with the experimental results received from the sensor during VOC sensing as discussed in Fig. 4. The post-layout simulation allowed to simulate the behaviour of the circuit including all parasitic resistances and capacitances introduced in the layout. The amplifier used is a two-stage folded cascode topology (Fig. 8(b)), which provides high gain and stability for a wide range of capacitive loads. The maximum output current is set at 63μA and this allows the use of small resistances (10 – 40k Ω). The simulated open-loop gain is 63dB, the -3dB bandwidth is 4 kHz, and the input-referred noise is 14.2 $\mu Vrms$ integrated from 1mHz to 4kHz.

However, an ADC is required in order to digitise and further post-process the digital signal at the cost of gradually increased design complexity. For that reason, different quasi-digital converters have been reported in literature including resistance-to-duty cycle, resistance–to-frequency, and resistance–to period, as they are simpler topologies, offering a wide dynamic range and a simplified interface to digital systems (e.g. microprocessors) [40]–[44].

Here, a quasi-digital readout circuit for applications that require gas detection is proposed. This circuit is a chemiresistive oscillator with target oscillating frequency at 13.56MHz allowing compatibility with passive near field communication tags, without the need of an ADC. As per post-layout simulations, the circuit can operate reliably up to 15MHz without the need of additional circuits for frequency locking. To validate the proposed approach, the circuit was designed, and post-layout simulated in the Cadence-Virtuoso environment at the 350nm CMOS technology. The block diagram of the proposed readout circuit is shown in Fig. 8.

The working principle of the proposed circuit is as follows: A switched capacitor (SC) network with variable capacitors is used instead of resistors allowing calibration of the system with digital controls. The SCs are chosen because they are easily configurable with digital controls, they have limited thermal noise compared to resistors and their temperature dependence is lower compared to resistors. The resistance of an SC can be calculated using the expression (Eq. 2):

$$R = 1/(C_x \cdot f) \tag{2}$$

where, C_x is the capacitance and f is the frequency of switching.. The detection is done in a pseudo-differential mode while applying a pulse (frequency 27.12MHz) at both inputs. This frequency can be applied using a crystal oscillator of the respective value. In the absence of a VOC both resistances R_{sens_ref} and R_{sens} have the same value and the output will be “High”. Once a VOC is introduced, the R_{sens} will start to deviate from R_{sens_ref} creating a change in the current and therefore a mismatch on the charging/discharging of the capacitive loads of each stage. This will cause a phase shift

TABLE II
PERFORMANCE COMPARISON OF DIFFERENT GAS/VOC SENSORS

Material	Type	Measurement Type	Replaceable	Bioresorbable	Operating Temp. (□C)	Response (%)	Ref
PEG-1540, PEG-20M, PEG-6000, and PVP	Polymer	Capacitive	No	No	-	~30	15
Ag@Fe_2O_3	Metal/Metal-oxide	Resistive	No	No	250	~6.3	20
Au@In_2O_3	Metal/Metal-oxide	Resistive	No	No	160	~36.14	21
V_2O_5 NWs	Metal-oxide	Resistive	No	No	330	~9.09	22
α-Fe_2O_3 NFs	Metal-oxide	Resistive	No	No	250	~12.5	23
Fe_2SO_4 aq. Sol.	Microfluidic	Resistive	Yes	No	RT	~50	12
NaCl aq Sol	Microfluidic	**Resistive**	**Yes**	**Yes**	**RT**	**20**	**This Work**

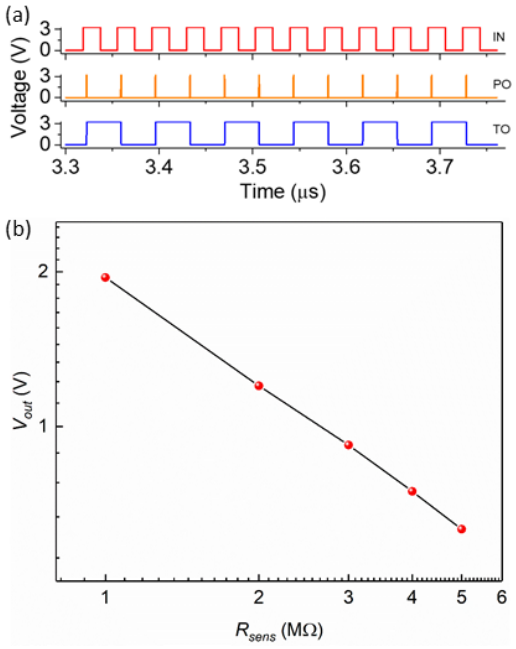

Fig. 9. (a) The input pulse (IN), the output of the PD (PO), and the toggled output (TO) for chemiresistance value at 3MΩ (b) the analogue output (V_{Out}) for different chemiresistance values shown in a log-log scale.

at the output of the inverters which can be detected from the phase detector (PD), whose output is finally toggled in order to create a 13.56MHz square wave pulse. The post-layout simulated input (IN), the output of the phase detector (PO), and the toggled output signals (TO) for chemiresistance 3M Ω are shown in Fig. 9(a). Based on post-layout simulations, when the chemiresistance is set at 3M Ω the output frequency stabilises after 3.25μs. Overall, the circuit can be used as an oscillator which can detect changes in the chemiresistance and it will start oscillating when R_{sense} falls below 3.8 M Ω. The analogue output can be recorded and correlated with the responses of volatile organic compounds, after undergoing calibration of the sensor. Fig. 9(b) shows the analogue output (V_{Out}) for the change in sensor resistance (R_{sens}). The analogue voltage can then be employed to detect organic vapours. Based on these simulated results we aim to fabricate in future the chips with electronics described above.

VI. CONCLUSION

A study was performed to check the capability of vapour sensing of a microdroplet based sensor. It was observed that the microdroplet require 1-2 seconds to stabilize on the flexible GOC substrate. The sensor showed responses for different organic vapours such as IPA, methanol, and ethanol due to the on-set of solutal Marangoni motion inside the droplet. The motion inside the droplet was related to the surface tension gradient between the air-water and vapour-water interface. The sensor showed a 14-21% change in resistance for the vapour exposures. The response time of the microdroplet-system was found to be 2-3 seconds. The GOC substrate was chosen due to biocompatibility and bioresorbability, which also make it suitable for disposable sensor applications. Additionally, the hydrogen bonds and electrostatic nature of GOC provides optimum hydrophobicity to the droplet system. The study was further extended to evaluate the effect of static bending, which is expected during practical usage. It was found that higher bending improved the response of the sensor due to the increase in the ratio of unexposed to the exposed surface of the droplet. Interestingly, these bending related changes indicate that bending could also be used to modulate the response of the sensor. The post-layout simulation of a readout circuit for chemiresistive quasi-digital oscillator is proposed with target oscillating frequency at 13.56MHz. The simulated response of the proposed circuit is also fast and stabilises after 3.25μs when the chemiresistance is set at 3M Ω. The total power consumption of the circuit is 1.58 mW. The input and conditions of the circuit were similar to the experimental response of the sensor. This study shows the possibility of the circuit to be implemented for the proposed microfluidic vapour sensor. The integration of the sensor with the proposed circuit and experiment with the same is kept as the future scope of this study.

ACKNOWLEDGMENT

The views and opinions in this document do not necessarily reflect those of the European Commission or the Special EU Programmes Body (SEUPB).

REFERENCES

[1] H. S. Kim, T. P. Devarenne, and A. Han, "Microfluidic systems for microalgal biotechnology: A review," *Algal Res.*, vol. 30, pp. 149–161, Mar. 2018.

[2] M. Yew, Y. Ren, K. S. Koh, C. Sun, and C. Snape, "A review of state-of-the-art microfluidic technologies for environmental applications: Detection and remediation," *Global Challenges*, vol. 3, no. 1, Jan. 2019, Art. no. 1800060.

[3] J. Panwar and R. Roy, "Integrated field's metal microelectrodes based microfluidic impedance cytometry for cell-in-droplet quantification," *Microelectronic Eng.*, vol. 215, Jul. 2019, Art. no. 111010.

[4] R. D. Sochol *et al.*, "3D printed microfluidics and microelectronics," *Microelectron. Eng.*, vol. 189, pp. 52–68, Apr. 2018.

[5] L. A. Fraser *et al.*, "A portable microfluidic aptamer-tethered enzyme capture (APTEC) biosensor for malaria diagnosis," *Biosensors Bioelectron.*, vol. 100, pp. 591–596, Feb. 2018.

[6] W. Dang, V. Vinciguerra, L. Lorenzelli, and R. Dahiya, "Printable stretchable interconnects," *Flexible Printed Electron.*, vol. 2, no. 1, Mar. 2017, Art. no. 013003.

[7] D. Thuau, C. Laval, I. Dufour, P. Poulin, C. Ayela, and J.-B. Salmon, "Engineering polymer MEMS using combined microfluidic pervaporation and micro-molding," *Microsyst. Nanoeng.*, vol. 4, no. 1, p. 15, Dec. 2018.

[8] R. Liu, N. Wang, F. Kamili, and A. F. Sarioglu, "Microfluidic CODES: A scalable multiplexed electronic sensor for orthogonal detection of particles in microfluidic channels," *Lab Chip*, vol. 16, no. 8, pp. 1350–1357, 2016.

[9] X. Weng, G. Gaur, and S. Neethirajan, "Rapid detection of food allergens by microfluidics ELISA-based optical sensor," *Biosensors*, vol. 6, no. 2, p. 24, 2016.

[10] V. B. Koman, T. T. S. Lew, M. H. Wong, S.-Y. Kwak, J. P. Giraldo, and M. S. Strano, "Persistent drought monitoring using a microfluidic-printed electro-mechanical sensor of stomata in planta," *Lab Chip*, vol. 17, no. 23, pp. 4015–4024, 2017.

[11] C. Carrell *et al.*, "Beyond the lateral flow assay: A review of paper-based microfluidics," *Microelectron. Eng.*, vol. 206, pp. 45–54, Feb. 2019.

[12] T. Akyazi, L. Basabe-Desmonts, and F. Benito-Lopez, "Review on microfluidic paper-based analytical devices towards commercialisation," *Analytica Chim. Acta*, vol. 1001, pp. 1–17, Feb. 2018.

[13] C.-Y. Lee, C.-L. Chang, Y.-N. Wang, and L.-M. Fu, "Microfluidic mixing: A review," *Int. J. Mol. Sci.*, vol. 12, no. 5, pp. 3263–3287, 2011.

[14] M. Bhattacharjee, V. Pasumarthi, J. Chaudhuri, A. K. Singh, H. Nemade, and D. Bandyopadhyay, "Self-spinning nanoparticle laden microdroplets for sensing and energy harvesting," *Nanoscale*, vol. 8, no. 11, pp. 6118–6128, 2016.

[15] P. Dak, A. Ebrahimi, V. Swaminathan, C. Duarte-Guevara, R. Bashir, and M. Alam, "Droplet-based biosensing for Lab-on-a-chip, open microfluidics platforms," *Biosensors*, vol. 6, no. 2, p. 14, 2016.

[16] M. Bhattacharjee, A. Vilouras, and R. Dahiya, "Microdroplet based organic vapour sensor on a disposable GO-Chitosan flexible substrate," in *Proc. IEEE Int. Conf. Flexible Printable Sensors Syst. (FLEPS)*, Jul. 2019, pp. 1–3.

[17] A. R. Indrapraja, M. Rivai, A. Arifin, and D. Purwanto, "The detection of organic solvent vapor by using polymer coated chemocapacitor sensor," *J. Phys., Conf. Ser.*, vol. 853, May 2017, Art. no. 012033.

[18] A. Mirzaei, S. G. Leonardi, and G. Neri, "Detection of hazardous volatile organic compounds (VOCs) by metal oxide nanostructures-based gas sensors: A review," *Ceram. Int.*, vol. 42, no. 14, pp. 15119–15141, Nov. 2016.

[19] S.-Y. Cho *et al.*, "High-resolution p-Type metal oxide semiconductor nanowire array as an ultrasensitive sensor for volatile organic compounds," *Nano Lett.*, vol. 16, no. 7, pp. 4508–4515, Jul. 2016.

[20] L. Manjakkal, B. Sakthivel, N. Gopalakrishnan, and R. Dahiya, "Printed flexible electrochemical pH sensors based on CuO nanorods," *Sens. Actuators B, Chem.*, vol. 263, pp. 50–58, Jun. 2018.

[21] M. Simić, L. Manjakkal, K. Zaraska, G. M. Stojanović, and R. Dahiya, "TiO_2-based thick film pH sensor," *IEEE Sensors J.*, vol. 17, no. 2, pp. 248–255, Jan. 2017.

[22] A. Mirzaei *et al.*, "Synthesis, characterization and gas sensing properties of Ag@α-Fe_2O_3 core–shell nanocomposites," *Nanomaterials*, vol. 5, no. 2, pp. 737–749, 2015.

[23] Y. Wang *et al.*, "Special nanostructure control of ethanol sensing characteristics based on Au@In_2O_3 sensor with good selectivity and rapid response," *RSC Adv.*, vol. 5, no. 13, pp. 9884–9890, 2015.

[24] W. Jin *et al.*, "Enhancement of ethanol gas sensing response based on ordered V_2O_5 nanowire microyarns," *Sens. Actuators B, Chem.*, vol. 206, pp. 284–290, Jan. 2015.

[25] S. G. Leonardi *et al.*, "A comparison of the ethanol sensing properties of α-iron oxide nanostructures prepared via the sol–gel and electrospinning techniques," *Nanotechnology*, vol. 27, no. 7, Feb. 2016, Art. no. 075502.

[26] L. Manjakkal, D. Shakthivel, and R. Dahiya, "Flexible printed reference electrodes for electrochemical applications," *Adv. Mater. Technol.*, vol. 3, no. 12, Dec. 2018, Art. no. 1800252.

[27] L. Manjakkal, A. Vilouras, and R. Dahiya, "Screen printed thick film reference electrodes for electrochemical sensing," *IEEE Sensors J.*, vol. 18, no. 19, pp. 7779–7785, Oct. 2018.

[28] W. Dang, L. Manjakkal, W. T. Navaraj, L. Lorenzelli, V. Vinciguerra, and R. Dahiya, "Stretchable wireless system for sweat pH monitoring," *Biosensors Bioelectron.*, vol. 107, pp. 192–202, Jun. 2018.

[29] L. Manjakkal, W. Dang, N. Yogeswaran, and R. Dahiya, "Textile-based potentiometric electrochemical pH sensor for wearable applications," *Biosensors*, vol. 9, no. 1, p. 14, 2019.

[30] X. Ren *et al.*, "A low-operating-power and flexible active-matrix organic-transistor temperature-sensor array," *Adv. Mater.*, vol. 28, no. 24, pp. 4832–4838, Jun. 2016.

[31] K. Luo, T. Huang, Y. Luo, H. Wang, C. Sang, and X. Li, "Thin film assembly of gold nanoparticles for vapor sensing via droplet interfacial reaction," *J. Mater. Sci. Technol.*, vol. 29, no. 5, pp. 401–405, May 2013.

[32] A. Vilouras, A. Paul, M. A. Kafi, and R. Dahiya, "Graphene oxide-chitosan based ultra-flexible electrochemical sensor for detection of serotonin," in *Proc. IEEE SENSORS*, Oct. 2018, pp. 1–4.

[33] M. A. Kafi, A. Paul, A. Vilouras, and R. Dahiya, "Mesoporous chitosan based conformable and resorbable biostrip for dopamine detection," *Biosensors Bioelectron.*, vol. 147, Jan. 2020, Art. no. 111781.

[34] M. W. Royal, N. M. Jokerst, and R. B. Fair, "Droplet-based sensing: Optical microresonator sensors embedded in digital electrowetting microfluidics systems," *IEEE Sensors J.*, vol. 13, no. 12, pp. 4733–4742, Dec. 2013.

[35] S.-Y. Teh, R. Lin, L.-H. Hung, and A. P. Lee, "Droplet microfluidics," *Lab Chip*, vol. 8, no. 2, pp. 198–220, 2008.

[36] M. A. Kafi, A. Paul, and R. Dahiya, "Graphene oxide-chitosan based flexible biosensor," in *Proc. IEEE SENSORS*, Oct. 2017, pp. 1–3.

[37] M. A. Kafi, A. Paul, A. Vilouras, and R. Dahiya, "Chitosan-graphene oxide based ultra-thin conformable sensing patch for cell-health monitoring," in *Proc. IEEE SENSORS*, Oct. 2018, pp. 1–4.

[38] A. Rianjanu, K. Triyana, D. B. Nugroho, A. Kusumaatmaja, and R. Roto, "Electrospun polyvinyl acetate nanofiber modified quartz crystal microbalance for detection of primary alcohol vapor," *Sens. Actuators A, Phys.*, vol. 301, Jan. 2020, Art. no. 111742.

[39] A. Rianjanu, D. B. Nugroho, A. Kusumaatmaja, R. Roto, and K. Triyana, "A study of quartz crystal microbalance modified with polyvinyl acetate nanofiber to differentiate short-chain alcohol isomers," *Sens. Bio-Sens. Res.*, vol. 25, Sep. 2019, Art. no. 100294.

[40] A. De Marcellis, C. Reig, and M.-D. Cubells-Beltrán, "A Capacitance-to-Time converter-based electronic interface for differential capacitive sensors," *Electronics*, vol. 8, no. 1, p. 80, 2019.

[41] K. Chuang Koay and P. Kwong Chan, "A 0.18-μm CMOS voltage-to-frequency converter with low circuit sensitivity," *IEEE Sensors J.*, vol. 18, no. 15, pp. 6245–6253, Aug. 2018.

[42] Z. Hijazi, M. Grassi, D. D. Caviglia, and M. Valle, "Time-based calibration-less read-out circuit for interfacing wide range MOX gas sensors," *Integration*, vol. 63, pp. 232–239, Sep. 2018.

[43] V. Sreenath, K. Semeerali, and B. George, "A resistive sensor readout circuit with intrinsic insensitivity to circuit parameters and its evaluation," *IEEE Trans. Instrum. Meas.*, vol. 66, no. 7, pp. 1719–1727, Jul. 2017.

[44] J. Lim, A. Rezvanitabar, F. L. Degertekin, and M. Ghovanloo, "An impulse radio PWM-based wireless data acquisition sensor interface," *IEEE Sensors J.*, vol. 19, no. 2, pp. 603–614, Jan. 2019.

Mitradip Bhattacharjee (Member, IEEE) received the B.Tech. degree in electronics and communication engineering from the National Institute of Technology, India, in 2013, and the Ph.D. degree from the Indian Institute of Technology, India, in 2018. He joined the Bendable Electronics and Sensing Technologies (BEST) Research Group, University of Glasgow, U.K., as a Postdoctoral Fellow in 2019. He is currently an Assistant Professor of Electrical Engineering and Computer Science with the Indian Institute of Science Education and Research Bhopal. His research interests include electronic sensors and systems, flexible/wearable and printed electronics, biomedical engineering, bioelectronics, and reconfigurable sensing antenna.

Anastasios Vilouras (Student Member, IEEE) received the B.Sc. degree in physics from the Aristotle University of Thessaloniki, Greece, in 2014, and the M.Sc. degree in bioelectronics and biosensors from the University of Edinburgh, U.K., in 2015. He is currently pursuing the Ph.D. degree with Bendable Electronics and Sensing Technologies (BEST) Group focusing mainly on CMOS-based bendable sensors for chemical and bio-chemical measurements with the University of Glasgow, U.K. He joined the Centre for Doctoral Training in Intelligent Sensing and Measurement (CDT-ISM), University of Glasgow, in 2016.

Ravinder Dahiya (Fellow, IEEE) is a Professor of Electronics and Nanoengineering with the University of Glasgow, U.K. He is the Leader of Bendable Electronics and Sensing Technologies (BEST) Research Group. His group conducts fundamental and applied research in the multidisciplinary fields of flexible and printed electronics, electronic skin, robotics and wearable systems. He has authored over 300 research articles, four books, and 15 submitted/granted patents. He is currently the President-Elect and the Distinguished Lecturer of the IEEE Sensors Council. He received the prestigious EPSRC fellowship, the Marie Curie Fellowship, and the Japanese Monbusho Fellowship. Among several awards, he received the 2016 Microelectronic Engineering Young Investigator Award and the 2016 Technical Achievement Award from the IEEE Sensors Council. He is serving on the Editorial Board of Scientific Reports. He was the Technical Program Co-Chair of the IEEE Sensors 2017 and 2018. He has been the General Chair of several conferences. He served on the Editorial Board for the IEEE SENSORS JOURNAL from 2012 to 2020, and the IEEE TRANSACTIONS ON ROBOTICS from 2012 to 2017.